

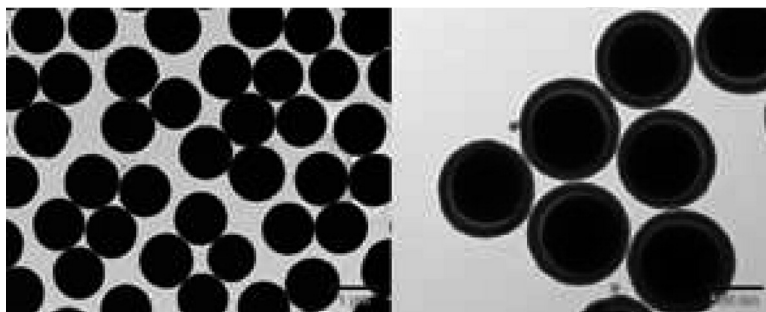
## Article

### Synthesis of Eccentric Titania/Silica Core/Shell and Composite Particles

Ahmet Faik Demirevs, Alfons van Blaaderen, and Arnout Imhof

*Chem. Mater.*, **2009**, 21 (6), 979-984 • DOI: 10.1021/cm803250w • Publication Date (Web): 25 February 2009

Downloaded from <http://pubs.acs.org> on March 25, 2009



#### More About This Article

Additional resources and features associated with this article are available within the HTML version:

- Supporting Information
- Access to high resolution figures
- Links to articles and content related to this article
- Copyright permission to reproduce figures and/or text from this article

[View the Full Text HTML](#)

## Synthesis of Eccentric Titania–Silica Core–Shell and Composite Particles

Ahmet Faik Demirörs,\* Alfons van Blaaderen, and Arnout Imhof\*

Soft Condensed Matter, Debye Institute for Nanomaterials Science, Department of Physics and Astronomy, Utrecht University, Princetonplein 5, 3584 CC Utrecht, The Netherlands

Received December 2, 2008. Revised Manuscript Received January 23, 2009

We describe a novel method to synthesize colloidal particles with an eccentric core–shell structure. Titania–silica core–shell particles were synthesized by silica coating of porous titania particles under Stöber (Stöber et al. *J. Colloid Interface Sci.* **1968**, 26, 62) conditions. We can control access of silica to the pores in the titania, allowing us to produce either core–shell or composite particles. Calcination of the core–shell particles gives unique eccentric core–shell structures, as a result of extensive shrinkage of the highly porous titania core with respect to the silica shell. However, when the titania particles are silica treated prior to drying they result in composite titania–silica spheres, where two materials are mixed uniformly. These spheres are interesting for catalysis, (switchable) photonic crystal applications, optical tweezing, and new titania based materials. We demonstrate photocatalytic activity of the eccentric spheres where the silica layer acts as a size selective membrane.

### 1. Introduction

The fabrication of functional hollow colloidal particles is of great scientific and technological interest with a wide range of applications, including drug delivery, coatings, photonic devices, and nanoscale reaction vessels.<sup>2–8</sup> Various methods, including approaches such as spray drying,<sup>9</sup> emulsion templating techniques,<sup>10,11</sup> and self-assembly processes,<sup>12</sup> have been described to prepare hollow spheres out of latex, metal, and inorganic materials.<sup>13–18</sup> Recently, much research has

been undertaken to functionalize the interior of the hollow spheres by encapsulation of metal nanoparticles.<sup>19–23</sup> Such an approach leads to the fabrication of unique catalytic systems. In particular, Arnal et al.<sup>13</sup> and Lee et al.<sup>24</sup> have shown that “rattle-like” core–shell particles have a much better catalytic performance compared to metal nanoparticles supported on the same material without a void in between. It was found that, in the case of eccentric core–shell particles, the core is effectively separated from other particles and also accessible to the gas molecules whereas in the no-void case mass transfer is limited within the microporous structure of the shell due to touching solid–solid interfaces. Eccentric particles also have the advantage of easier heat treatment without causing any aggregation of the encapsulated ingredient even under harsh reaction conditions. This feasibly leads to high catalytic activity because aggregation, usually caused by coalescence of the particles or Ostwald ripening, is known to result in loss of catalytic activity.<sup>25</sup>

Hollow particles equipped with functional microparticles also offer an opportunity for size-selective catalysis. Ikeda

\* Corresponding authors. E-mail a.f.demirors@uu.nl, tel. +31 30 253 2315, fax +31 30 253 2706 (A.F.D.); E-mail a.imhof@uu.nl, tel +31 30 253 2423 (A.I.).

- (1) Stöber, W.; Fink, A.; Bohn, E. *J. Colloid Interface Sci.* **1968**, 26, 62.
- (2) Pekarek, K. J.; Jacob, J. S.; Mathiowitz, E. *Nature* **1994**, 367, 258.
- (3) Liang, H. P.; Zhang, H. M.; Hu, J. S.; Guo, Y. G.; Wan, L. J.; Bai, C. L. *Angew. Chem., Int. Ed.* **2004**, 116, 1566.
- (4) Zhu, Y.; Shi, J.; Shen, W.; Dong, X.; Feng, J.; Ruan, M.; Li, Y. *Angew. Chem., Int. Ed.* **2005**, 117, 5213.
- (5) Li, J.; Zeng, H. C. *Angew. Chem., Int. Ed.* **2005**, 117, 4416.
- (6) Chen, J. Y.; Wiley, B.; Li, Z. Y.; Campbell, D.; Saeki, F.; Cang, H.; Au, L.; Lee, J.; Li, X. D.; Xia, Y. N. *Adv. Mater.* **2005**, 17, 2255.
- (7) Shchukin, D. G.; Sukhorukov, G. B. *Adv. Mater.* **2004**, 16, 671.
- (8) Lou, X. W.; Yuan, C.; Archer, L. A. *Adv. Mater.* **2007**, 19, 3328.
- (9) Lu, Y.; Fan, H.; Stump, A.; Ward, T. L.; Rieker, T.; Brinker, C. J. *Nature* **1999**, 398, 223.
- (10) Schacht, S.; Huo, Q.; Voigt-Martin, I. G.; Stucky, G. D.; Schuth, F. *Science* **1996**, 273, 768.
- (11) Thurmond, K. B.; Kowalewski, T.; Wooley, K. L. *J. Am. Chem. Soc.* **1997**, 119, 6656.
- (12) Discher, B. M.; Won, Y. Y. D. S.; Ege, J.; Lee, C. M.; Bates, F. S.; Discher, D. E.; Hammer, D. A. *Science* **1999**, 284, 1143.
- (13) Arnal, P. M.; Comotti, M.; Schuth, F. *Angew. Chem., Int. Ed.* **2006**, 45, 8224.
- (14) Zhong, Z.; Yin, Y.; Gates, B.; Xia, Y. *Adv. Mater.* **2000**, 12, 206.
- (15) Wu, D.; Ge, X.; Zhang, Z.; Wang, M.; Zhang, S. *Langmuir* **2004**, 20, 5192.
- (16) Chen, Z.; Zhan, P.; Wang, Z.; Zhang, J.; Zhang, W.; Ming, N.; Chan, C. T.; Sheng, P. *Adv. Mater.* **2004**, 16, 417.

- (17) Pavlyuchenko, V. N.; Srochinskaya, O. V.; Ivanchev, S. S.; Klubin, V. V.; Kreichman, G. S.; Budtov, V. P.; Skrifvars, M.; Halme, E.; Koskinen, J. *J. Polym. Sci., Polym. Chem.* **2001**, 39, 1435.
- (18) Caruso, F.; Caruso, R. A.; Möhwald, H. *Science* **1998**, 282, 1111.
- (19) Kim, M.; Sohn, K.; Bin, Na, H.; Hyeon, T. *Nano Lett.* **2002**, 12, 1383.
- (20) Hah, H. J.; Um, J. I.; Han, S. H.; Koo, S. M. *Chem. Commun.* **2004**, 1012.
- (21) Cheng, D.; Zhou, X.; Xia, H.; Chan, H. S. O. *Chem. Mater.* **2005**, 17, 3578.
- (22) Zhang, K.; Zhang, X.; Chen, H.; Chen, X.; Zheng, L.; Zhang, J.; Yang, B. *Langmuir* **2004**, 20, 11312.
- (23) Kim, J. Y.; Yoon, S. B.; Yu, J. S. *Chem. Commun.* **2003**, 790.
- (24) Lee, J.; Park, J. C.; Song, H. *Adv. Mater.* **2008**, 20, 1523.
- (25) Harris, P. J. F. *J. Catal.* **1986**, 97, 527.

et al. demonstrated that titania encapsulated by a silica shell can be used for size-selective photocatalytic decomposition of organics.<sup>26,27</sup> The pore sizes in the silica shell determine the size selectivity: molecules larger than the silica pore size are filtered out and not catalyzed while smaller molecules are. This approach may lead to important applications combined with the knowledge that the silica pore size can be finely tuned from mesoporous (2–50 nm) to microporous (<2 nm) by modifying the synthesis conditions of silica.<sup>28,29</sup>

Monodisperse eccentric particles with movable cores have been suggested for photonic crystals tunable by an external field.<sup>30</sup> Such particles due to their monodisperse spherical outer shell can form ordered crystals but because of the random distribution of the core particles will not have a photonic band gap. Camargo et al.<sup>30</sup> demonstrated by computation that an external field that aligns particles along field lines can cause a band gap to open as a result of the induced long-range order. This approach brings also the chance of tuning the gap position by changing an external field strength.<sup>31</sup>

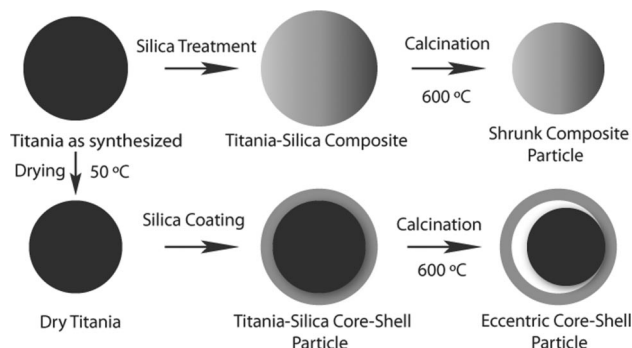
Reports for the preparation of eccentric particles are mostly based on successive two step coating of the core particle and sacrificial removal of the middle shell.<sup>8,13,30,32</sup> Here we report a novel and shorter way of fabricating eccentric core-shell particles by taking advantage of porous titania particles that upon sintering shrink much more than the silica shell enclosing them. We also show that control over the access of silica to the pores can be used to produce either core-shell or composite particles. We believe that our approach constitutes a new way of manipulating the morphology of composite particles and can be used to synthesize new types of composite particles based on titania.

## 2. Experimental Section

The synthesis of the titania particles was done according to the procedure of Eiden-Assmann et al.<sup>33</sup> In a typical synthesis, 250 mL of ethanol with 17.0 mL of  $\text{Ti}(\text{OC}_2\text{H}_5)_4$  was mixed with 750 mL of ethanol with 4.0 mL of 0.1 M aqueous Lutensol ON50 (BASF) solution. This gives monodisperse titania particles with a size between 900–1200 nm depending on the reaction temperature and the amount of the titania precursor. The titania particles are then collected by centrifugation.

After being dried in an oven at 50 °C for 2 h the particles are coated with silica under Stöber conditions. Typically 0.082 g of titania was dispersed in 50 mL of ethanol, and 0.55 mL of ammonia was added to the dispersion. It was followed by 0.8 mL of tetraethoxysilane (TEOS) and, if desired, a suitable amount of [3-aminopropyl]trimethoxysilane (APS) coupled to rhodamine isothiocyanate (RITC) for fluorescent labeling the silica (0.02 g

### Scheme 1. Schematic Representation of the Procedure for Fabrication of *comp*- $\text{TiO}_2@/\text{SiO}_2$ , *cs*- $\text{TiO}_2@/\text{SiO}_2$ , and *ecc*- $\text{TiO}_2@/\text{SiO}_2$ Particles



APS and 0.005 RITC for 1 mL of TEOS).<sup>34</sup> The particles were then coated with extra silica (without dye) in 100 mL of ethanol with 5 mL of ammonia and 2 mL of TEOS. Silica coating of the dried titania results in *cs*- $\text{TiO}_2@/\text{SiO}_2$  particles. Upon calcination at 600–625 °C for 15–60 min the *cs*- $\text{TiO}_2@/\text{SiO}_2$  particles give rise to *ecc*- $\text{TiO}_2@/\text{SiO}_2$  particles. Exactly the same procedure, except for the drying step at 50 °C, was followed to produce the *comp*- $\text{TiO}_2@/\text{SiO}_2$  particles.

Static Light Scattering was performed with home-built equipment using a He–Ne laser as a light source (632.8 nm, 10 mW). The logarithm of scattering intensity data were plotted against the scattering vector  $k = 4 \pi n \sin(\theta/2)/\lambda$ , where  $n$  is the solvent refractive index,  $\theta$  is the scattering angle, and  $\lambda$  the wavelength in vacuum.

The powder XRD measurements were performed with a Philips PW 1820 diffractometer with a Philips PW 1729 X-ray generator (Cu  $K_\alpha$  radiation). In the photocatalysis experiments a 6W Hg UV lamp with a wavelength of 251 nm was used. Uncapped scintillation vials were used with 15 mg of titania dispersed in 10 mL of aqueous solution containing 0.61  $\mu\text{mol}$  Methylene Blue (MB), 0.34  $\mu\text{mol}$  RITC or 0.20  $\mu\text{mol}$  RITC in RITC-PAH sample. RITC was coupled to poly(allylamine hydro-chloride) (PAH) according to the procedure of Donath et al.<sup>35</sup>

## 3. Results and Discussion

The route for the fabrication of composite (*comp*- $\text{TiO}_2@/\text{SiO}_2$ ), core-shell (*cs*- $\text{TiO}_2@/\text{SiO}_2$ ) and eccentric core-shell (*ecc*- $\text{TiO}_2@/\text{SiO}_2$ ) titania-silica particles is given in Scheme 1. After being dried in an oven at 50 °C for 2 h, titania particles can be coated with silica under Stöber conditions.<sup>1</sup> We also couple the fluorescent dye rhodamine isothiocyanate (RITC) to silica.<sup>34</sup> Silica coating of the dried titania results in *cs*- $\text{TiO}_2@/\text{SiO}_2$  particles. Upon calcination at 600–625 °C for 15–60 min the titania cores of *cs*- $\text{TiO}_2@/\text{SiO}_2$  particles shrink more because of higher porosity of the titania compared to silica giving rise to *ecc*- $\text{TiO}_2@/\text{SiO}_2$  particles. On the other hand, it was observed that the titania particles are very sensitive to the drying step. If the drying step was omitted the as-synthesized particles upon silica treatment formed homogeneously mixed *comp*- $\text{TiO}_2@/\text{SiO}_2$  particles.

(26) Ikeda, S.; Ikoma, Y.; Kobayashi, H.; Harada, T.; Torimoto, T.; Ohtani, B.; Matsumura, M. *Chem. Commun.* **2007**, 3753.

(27) Ikeda, S.; Kobayashi, H.; Ikoma, Y.; Harada, T.; Torimoto, T.; Ohtani, B.; Matsumura, M. *Phys. Chem. Chem. Phys.* **2007**, 9, 6319.

(28) Behrens, P. *Adv. Mater.* **1993**, 5, 127.

(29) Lu, Z.; Xu, J.; Han, Y.; Song, Z.; Li, J.; Yang, W. *Colloids Surf., A* **2007**, 303, 207.

(30) Camargo, P. H. C.; Lib, Z. Y.; Xia, Y. *Soft Matter* **2007**, 3, 1215.

(31) Ge, J.; Hu, Y.; Yin, Y. *Angew. Chem., Int. Ed.* **2007**, 46, 7428.

(32) Lou, X. W.; Yuan, C.; Archer, L. A. *Small* **2007**, 3, 261.

(33) Eiden-Assmann, S.; Widoniak, J.; Maret, G. *Chem. Mater.* **2004**, 16, 6.

(34) van Blaaderen, A.; Vrij, A. *Langmuir* **1992**, 8, 2921.

(35) Schnackel, A.; Hiller, S.; Reibetanz, U.; Donath, E. *Soft Matter* **2007**, 3, 200.

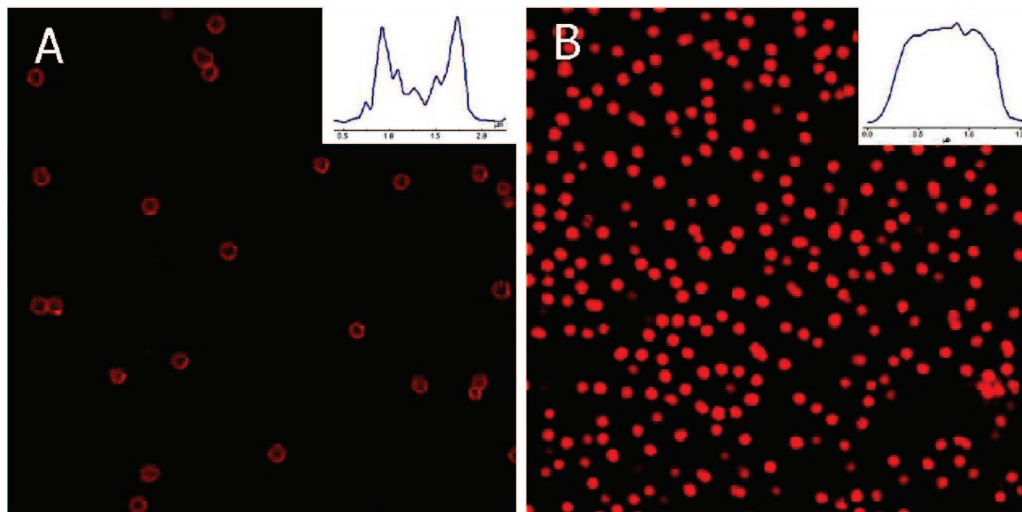


**Figure 1.** Confocal fluorescence microscopy images of titania–silica particles: (a) *cs*-TiO<sub>2</sub>@SiO<sub>2</sub> produced by drying in an oven for 2 h at 50 °C followed by silica coating (image size 37.5 μm × 37.5 μm) and (b) the same titania particles without drying which forms *comp*-TiO<sub>2</sub>@SiO<sub>2</sub> particles upon silica treatment. Insets are line profiles through single particles (image size 47.25 μm × 47.25 μm).

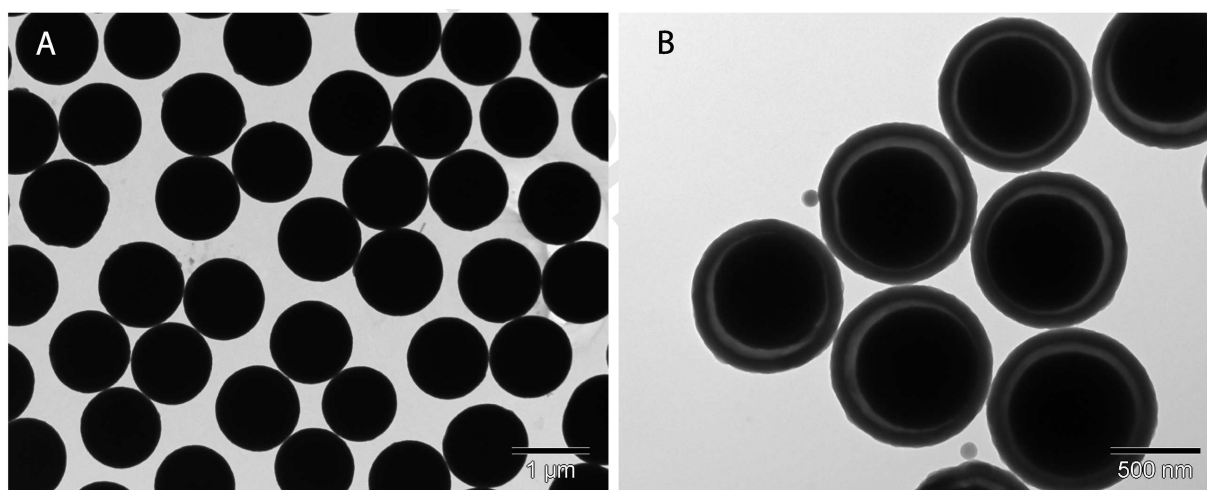


**Figure 2.** TEM images of the titania particles: (a) titania particles as synthesized and (b) eccentric titania–silica core–shell particles after calcination.

The striking influence of the drying step can be appreciated by comparing the confocal fluorescence microscopy images. For the *cs*-TiO<sub>2</sub>@SiO<sub>2</sub> particles we observe a ring-like structure which demonstrates the core–shell structure of the particle where only the fluorescently labeled silica coating is visible in Figure 1a. However, in the case of *comp*-TiO<sub>2</sub>@SiO<sub>2</sub> particles in Figure 1b the image shows a fully dyed structure, which means that RITC dye (coupled to silica) is dispersed throughout the particle on a nanometer scale. The insets show line profiles on a single particle and show the properties of core–shell and fully dyed structures.

A TEM micrograph of the bare titania particles is given in Figure 2a. The *ecc*-TiO<sub>2</sub>@SiO<sub>2</sub> particles shown in Figure 2b were synthesized by taking advantage of the high porosity of the core titania particles. The core titania particles shrunk upon calcination and formed *ecc*-TiO<sub>2</sub>@SiO<sub>2</sub> particles. For the case shown in Figure 2a we found the size of the eccentric particles to be 850 nm (5% polydispersity) and the shell thickness to be 70 nm, where the inner core was 630 nm. The void between the shrunk core and the silica shell was

around 40–120 nm depending on the particle size and the calcination time.

As further support for our interpretation of the particle structure we performed energy dispersive X-ray (EDX) analysis for the *comp*-TiO<sub>2</sub>@SiO<sub>2</sub> and *ecc*-TiO<sub>2</sub>@SiO<sub>2</sub> particles. Figure 3a shows the EDX line graph of a *comp*-TiO<sub>2</sub>@SiO<sub>2</sub> particle obtained in STEM mode by performing the scan shown in Figure 3b. It is observed that both the silicon and titanium peaks start at the same radial position and have the same profile across the particle, which corresponds to that of a spherical object. This verifies that silica is dispersed throughout the particle homogeneously. In the case of *ecc*-TiO<sub>2</sub>@SiO<sub>2</sub> particles the EDX line graph in Figure 3c clearly demonstrates the eccentric core–shell structure with silicon showing the characteristic shell peaks on the ends.<sup>36</sup> Note that titanium shows up after silicon and exists only in the inner part of the particle. Importantly, there

(36) Zoldesi, C. I.; Imhof, A. *Adv. Mater.* **2005**, *17*, 924.

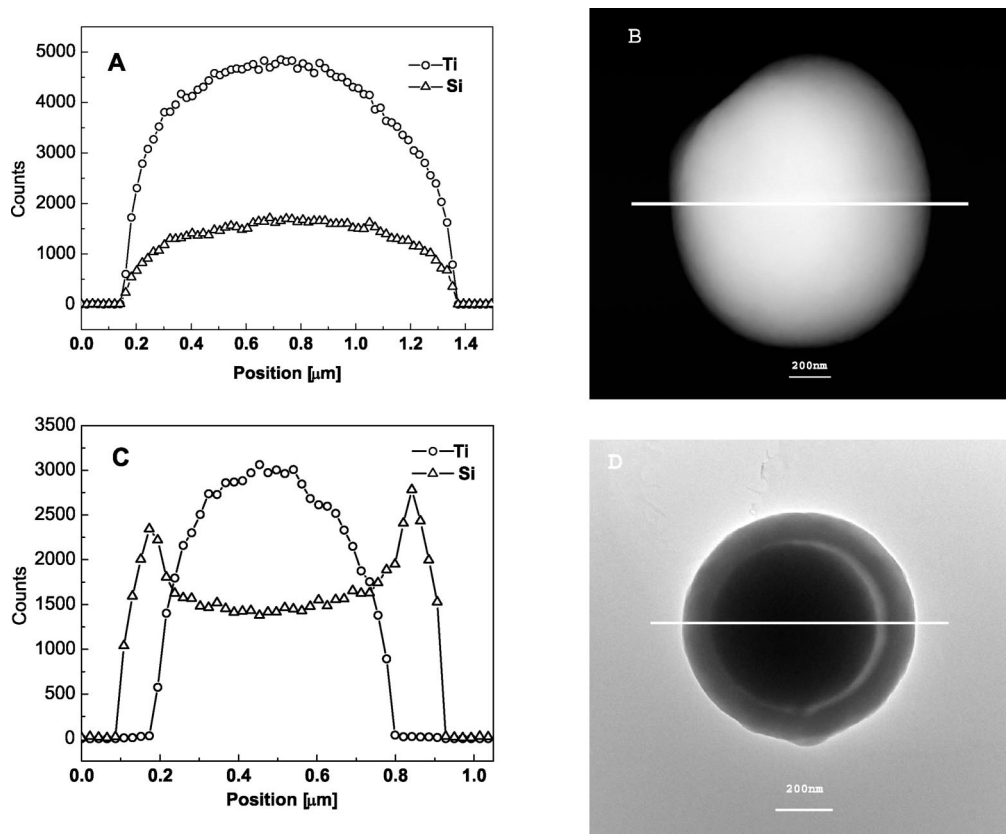


**Figure 3.** (a) EDX line graph of a composite titania-silica particle obtained in STEM mode by performing the scan shown in b and (b) TEM dark-field image showing the EDX line-scan through the composite particle (scan was performed from left to right). (c) EDX line graph of an eccentric titania-silica core-shell particle obtained in STEM mode by performing the scan shown in d and (d) TEM image showing the EDX line-scan through the eccentric core-shell particle.

is a 45 nm gap between the silicon peak and the point where titanium ends, which is due to the space between the titania core and the silica shell (see Supporting Information Figure S1).

Silica coating of the particles increases their size; as for dried titania the silica only coats the surface of the particle, and thus particle growth is mainly on the surface. However, we observed larger particle sizes (1.3  $\mu\text{m}$ ) for the silica treated particles without drying compared to dried ones (1.1  $\mu\text{m}$  where bare particles were 1.0  $\mu\text{m}$ ), although we otherwise applied the same treatment to both batches. We believe that prior to drying the particles are in a swollen state and, upon silica treatment, are filled with the added silica. In other words, the swollen particles upon drying shrink to a less porous state, but silica filling of the pores prevents this shrinkage. The dried particles shrink further upon calcination due to the still high porosity of the particles with a specific surface area of 300  $\text{m}^2/\text{g}$ .<sup>33</sup> We have shown the large effect of drying and sintering on the titania particles size by static light scattering (SLS).

Figure 4 shows the data compared to the Mie scattering calculations for a uniform sphere.<sup>37</sup> The locations of the minima and maxima on the  $k$ -axis depend sensitively on the

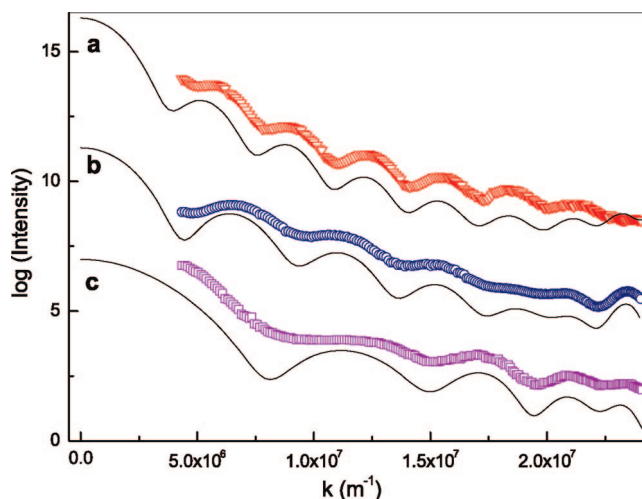


**Figure 4.** SLS experimental curves of the titania particles (symbols) in ethanol fitted to theoretical calculations of the full Mie solutions to the form factor (lines, offset for clarity): (a) titania particles as synthesized, radius 900 nm, refractive index 1.63, (b) titania particles after drying, radius 675 nm, refractive index 1.8, and (c) titania particles after calcination at 650  $^{\circ}\text{C}$ , radius 525 nm, refractive index 2.3, all curves are fitted for 4% polydispersity ( $k$  = scattering vector).

particle size and refractive index, whereas the depth of the minima gives an estimate of the polydispersity.<sup>38</sup> Curve a in Figure 4 is the SLS curve for the as-synthesized titania particles fitted to the full Mie solutions of the form factor

(37) Bohren, C. F.; Huffman, D. R. *Absorption and Scattering of Light by Small Particles*; Wiley: New York, 1983.

(38) Kerker, M.; Farone, W. A.; Smith, L. B.; Matijevic, E. *J. Colloid Sci.* **1964**, *19*, 193.

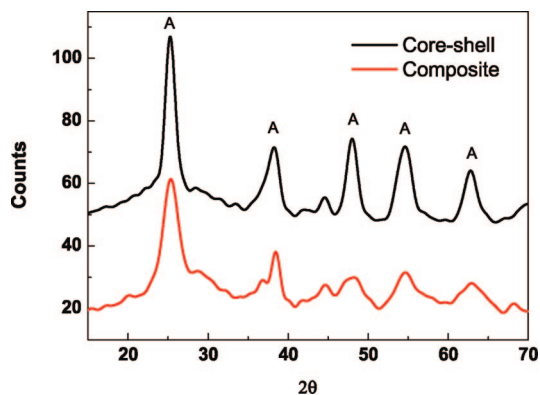


**Figure 5.** XRD pattern of the calcined *cs*-TiO<sub>2</sub>@SiO<sub>2</sub> particles (upper, 620 °C for 25 min) and the calcined titania–silica composite particles (lower, 620 °C for 60 min). Typical anatase peaks are denoted with “A”.

with radius and refractive index of 900 nm and 1.63, respectively. The SLS curves b and c belong to the dried and 650 °C sintered titania (bare) particles. The Mie fitting for these samples give 675 and 525 nm for radii and 1.8<sup>39</sup> and 2.3 for the refractive indices, respectively. The SLS curves clearly show the extensive shrinkage of the particle through the drying and calcination steps even by mere inspection of the number of the minima in the curves, which decreases from 7 (1.8 μm, as synthesized) to 6 (1.35 μm, dried) to 4 (1.05 μm, calcined). The large size difference between the nondried and dried particles explains why we get two different types of particles upon silica treatment. Titania particles as-synthesized have a tenuous structure and are not fully condensed, so before drying they clearly have a very open network which is accessible to the silica precursors (even to silica oligomers). We expect that due to this property the nondried particles are accessible to many types of chemicals, which opens a way to synthesize mixed composite particles by adding other precursors. On the other hand, drying closes up the titania network and densifies the matrix, such that silica can no longer penetrate into the particles but accumulates on their surfaces.

Amorphous titania synthesized with the sol–gel method is known to exhibit phase transitions upon heating. X-ray diffraction (XRD, Figure 5 and Supporting Information, Figure S2) measurements show that the particles become anatase in crystal structure even upon short heat treatments, like 15–20 min at 600 °C. The structure turns to rutile upon longer calcinations at 1000 °C. The crystallite size of the samples was estimated with the Debye–Scherrer equation  $t = 0.9\lambda / (B \cos \theta_B)$  where  $t$  is the average size of the crystalline domains,  $\lambda$  is the wavelength of the X-ray source, 1.5403 Å,  $B$  is the full width half maximum of the XRD line in radians, and  $\theta_B$  is half the angle of the XRD peak. The composite particles had a significantly smaller crystallite size than core–shell particles. Apparently, the presence of silica in the pores of the titania prevents crystallite domain growth. This also suggests that silica is well dispersed in the particle at the nanometer level. We found a crystallite

**Table 1.** BET Surface Area, BJH Pore Size, and Total Pore Volumes of the Titania Particles before Calcination

sample	N <sub>2</sub> BET (m <sup>2</sup> /g)	BJH pore size (nm)	pore vol. (cm <sup>3</sup> /g)
<i>comp</i> -TiO <sub>2</sub> @SiO <sub>2</sub>	273	1.68	0.151
<i>cs</i> -TiO <sub>2</sub> @SiO <sub>2</sub>	202	1.93	0.117
bare TiO <sub>2</sub>	232	1.76	0.128
silica	3	4.9	0.0062

size for the core–shell particles of 5 nm after 25 min of calcination at 620 °C and 3 nm for the composite particles after 60 min of calcination at the same temperature. Considering that crystallite size increases with calcination time, this difference is significant. When the calcination time was increased to 12 h, the crystallite sizes grew to 9 and 5 nm for core–shell and composite particles, respectively.

The crystallite size for bare titania grew even faster; after calcination at 620 °C for 25 min a size of 11 nm was found. We think that this difference is because of the silica shell which slows down the burning process of residual organic material in the titania and increases the time for crystal growth. It should also be noted that we have observed longer calcination times for thicker silica coated particles.

Nitrogen adsorption/desorption isotherms of the particles were measured to further investigate the porosity of the particles. They were of type I (microporous) except for pure silica colloids which were type II (nonporous). Brunauer–Emmett–Teller (BET) surface area, Barret–Joyner–Halenda (BJH) adsorption average pore diameter, and total pore volume of the samples before calcination are tabulated in Table 1. For comparison, data on silica colloids prepared by the Stöber method are also included. The particles were all degassed at 150 °C prior to the adsorption measurements, unfortunately making it impossible to do an independent measurement on nondried titania. Surprisingly, the *comp*-TiO<sub>2</sub>@SiO<sub>2</sub> particles had a much higher surface area and pore volume than both the bare titania and the core–shell particles. We believe that this is due to the presence of the silica dispersed throughout the particle, which cements the titania together allowing it to preserve its porosity during the drying step.

High surface area is a crucial parameter for catalytic applications of titania which is well-known for its photocatalytic properties. Although inorganic supports have been used for size-selective photocatalytic purposes they have always faced the difficulty of preserving the activity of the initially active photocatalyst.<sup>25</sup> Recently, it was shown that a catalyst with a void between the core and the shell catalytically may perform better than their no-void core–shell counterparts as they are able to retain the catalytic activity of the starting catalyst.<sup>13,27</sup> Our *ecc*-TiO<sub>2</sub>@SiO<sub>2</sub> particles have similar structure and can be suitable for size-selective catalysis. To demonstrate the size-selectivity, the photocatalytic activity was evaluated by degradation of various substrates with different sizes in aqueous suspensions. Typical results are summarized in Table 2. In the degradation of methylene blue (MB) and RITC which are relatively large (MB is 1.43 nm × 0.61 nm × 0.4 nm),<sup>40</sup> eccentric particles show mildly lower activity compared to the bare particles. However, the degradation of the large substrate poly(ally-

(39) Lee, S. H.; Roichman, Y.; Yi, G. R.; Kim, S. H.; Yang, S. M.; van Blaaderen, A.; van Oostrum, P.; Grier, D. G. *Opt. Express* **2007**, *15*, 18275.

(40) Costas, P.; Snoeyink, V. L. *Carbon* **2000**, *38*, 1423.

**Table 2. Photocatalytic Degradation of MB and RITC with Bare, Eccentric, and Composite Titania Particles**

sample	exposure time, h	MB or RITC decomposed
TiO <sub>2</sub>	20	0.61 μmol MB
Ecc-TiO <sub>2</sub>	20	0.29 μmol MB
Commercial TiO <sub>2</sub> <sup>a</sup>	1	0.65 μmol MB
SiO <sub>2</sub> /void/TiO <sub>2</sub> <sup>a</sup>	1	0.34 μmol MB
TiO <sub>2</sub>	18	0.34 μmol RITC
ecc-TiO <sub>2</sub>	18	0.19 μmol RITC
TiO <sub>2</sub>	20	0.21 μmol RITC-PAH
ecc-TiO <sub>2</sub>	20	0.03 μmol RITC-PAH

<sup>a</sup> Data is taken from ref 27 for comparison.

lamine hydrochloride) (PAH; MW = 15 000) coupled to RITC is almost completely suppressed by the silica shell. Additionally, in a mixture of ethanol and RITC-PAH we observed no change at all in the absorbance of the RITC which means that only ethanol was selectively degraded and the silica shell blocked the degradation of the large RITC-PAH. The suppression of photocatalytic activity for the degradation of relatively large molecules compared to the activity of bare titania indicates that these particles are promising for designing photocatalysts with molecular size selectivity.

Another point of interest for the *ecc*-TiO<sub>2</sub>@SiO<sub>2</sub> particles is their regular shape with a sphericity factor of 1.03 and low polydispersity of around 5% (measured by image analysis on TEM images), which gives them the ability to form colloidal crystals. The confocal microscopy image in Figure 6 of *cs*-TiO<sub>2</sub>@SiO<sub>2</sub> particles dried from a drop of suspension on a glass microscope slide exhibit 2D hexagonal order, and together with the SLS curves in Figure 4 suggest that our system should be monodisperse enough for photonic crystal applications. In a colloidal crystal of eccentric particles the cores will be randomly oriented in the absence of an external field. However, an external field may be used to rotate the particles into alignment with the field lines leading to tunability of the band gap.<sup>30,31</sup> We are currently investigating this possibility further.

#### 4. Conclusion

We have reported an easy self-templated way of fabricating colloidal eccentric particles and composite particles. This

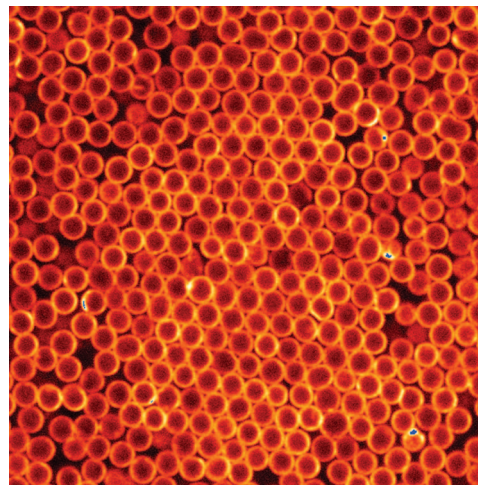


**Figure 6.** Confocal microscopy images of *cs*-TiO<sub>2</sub>@SiO<sub>2</sub> particles labeled with RITC dried on a glass microscope slide [Image size 37.5 μm × 37.5 μm].

approach produces eccentric particles directly from titania microspheres coated with silica, eliminating the need for costly and time-consuming sacrificial shell-removing steps associated with other procedures. Controlling the access of silica to the pores in the titania offers the flexibility of obtaining various types of particles with important applications in photonic crystals and photocatalysis. Additionally, *comp*-TiO<sub>2</sub>@SiO<sub>2</sub> particles give the opportunity of tuning particle properties like density and refractive index by tuning the fraction of silica added to the titania particle. Controlling pore access should be possible for materials other than silica as well and could lead to a whole range of functional composite particles. Currently we are working on producing colloidal BaTiO<sub>3</sub> and SrTiO<sub>3</sub> particles from Ba and Sr salts using this approach.

**Acknowledgment.** The authors thank J.D. Meeldijk for the assistance with the EDX measurements and Andrew I. Campbell for fruitful discussions.

**Supporting Information Available:** EDX graph of eccentric particles and XRD of calcined particles (PDF). This information is available free of charge via the Internet at <http://pubs.acs.org>.

CM803250W